Journal of Materials Chemistry C

ROYAL SOCIETY OF CHEMISTRY

REVIEW

View Article Online
View Journal | View Issue

Cite this: J. Mater. Chem. C, 2022, 10, 13312

Recent progress in polymer-based infrared photodetectors

Dongyang Zhu,[a] Deyang Ji, *[a] Liqiang Li [a] and Wenping Hu[bc]

Received 16th February 2022,
Accepted 27th March 2022

DOI: 10.1039/d2tc00646d

rsc.li/materials-c

Infrared (IR) photodetectors (PDs) have developed rapidly due to their potential applications in remote sensing, infrared imaging, and biomedical testing. The designable molecular structure, solution processability, large-area preparation, and intrinsic flexibility of polymer materials make it a potential material for a new generation of IR PDs. Through different molecular design strategies and innovative device architectures, the performance of PDs is optimized, and its application scenarios are expanded, which further promotes the rapid development of IR PDs. In this review, we summarized the development and recent progress of polymer-based organic photodiodes (OPDIs) and organic phototransistors (OPTs) including the brief mechanism and design strategy. Also, the challenges and perspectives of infrared photodetectors are presented, aiming to provide researchers with new design ideas and promote their further development.

1. Introduction

Infrared photodetectors, converting incident infrared light with a wavelength greater than 780 nm into electrical signals to realize the sensing of optical signals, have been greatly developed and shown promising applications in night vision, face recognition, intelligent sorting, blood oxygen detection, medical imaging, weather forecast, molecular chemistry, and infrared communication, *etc.*[1–8] In order to have a sufficient response to longer wavelength infrared light, infrared detectors must use semiconductor materials with narrow optical band gaps as photosensitive materials, which can allow low-energy photons to generate excitons, but this also results in a low carrier migration rate and high defect density.[7,9–12] So far, traditional inorganic materials with a stable and superior performance as semiconductor active layers, have achieved a certain degree of commercialization.[13,14] However, the processing of these materials has to be realized by high temperature, high pressure, or high vacuum and other complex process methods, resulting in the increase of the difficulty and cost of

[a] Tianjin Key Laboratory of Molecular Optoelectronic Sciences, Department of Chemistry, Institute of Molecular Aggregation Science, Tianjin University, Tianjin 300072, China. E-mail: jideyang@tju.edu.cn
[b] Tianjin Key Laboratory of Molecular Optoelectronic Sciences, Department of Chemistry, School of Science, Tianjin University, Collaborative Innovation Center of Chemical Science and Engineering, Tianjin 300072, China
[c] Haihe Laboratory of Sustainable Chemical Transformations, Tianjin 300192, China

Dongyang Zhu

Dongyang Zhu received his bachelor's degree from the University of Jinan, China in 2018 and his master's degree from Qingdao University of China in 2021. Now he is studying for a PhD under the supervision of Prof. Deyang Ji. His research interest focuses on organic optoelectronics.

Deyang Ji

Deyang Ji is a professor in Institute of Molecular Aggregation Sciences, Tianjin University. He received his B.S. from the Ocean University of China in 2009. He received his PhD from the Institute of Chemistry, Chinese Academy of Sciences in 2014 under the supervision of Prof. Wenping Hu. And then he did his research as a postdoc fellow in the group of Prof. Harald Fuchs in University of Münster, Germany. In 2019, he joined Tianjin University as a Professor. His research interest focuses on organic optoelectronics.

production.[15–17] To this end, the emergence and development of polymer materials offer better-performing alternatives.[3,18–21] Polymer semiconductors can be pre-molecularly designed to achieve desired functions, and this feature could expand their application scenarios.[22] Moreover, polymer semiconductors are solution processable and have the potential for large-area printing, which greatly reduces the process difficulty and cost of polymer semiconductors in device preparation.[2,5,6,23] The intrinsic flexibility of polymer materials provides the necessary prerequisites for the realization of flexible devices, and lays the foundation for the development of infrared detectors into wearable devices.[24–26] Expectedly, with the advantages of highly tunable optoelectronic properties, economical large-area deposition and low-temperature processing, polymer materials have extended the spectral range of these materials beyond visible light, making the application in infrared photodetectors more promising. Infrared light-sensitive polymers and their molecular structures mentioned in this review are summarized in Scheme 1.

Here, we aim to mainly discuss the recent progress of polymer-based photodiodes and phototransistors. Since the working mechanism of organic photodiodes (OPDIs) and organic phototransistors (OPTs) have already been reviewed by a number of authors,[2,27,28] we will not cover this part here. After a brief introduction in this section, the second section will summarize the infrared photodiodes with a polymer active layer and the use of mixed polymer/inorganic materials as the active layer. The third section will discuss the latest developments in infrared phototransistors using polymer semiconductor layers, polymer/inorganic material channel layers, and polymers as dielectric layers. An overview of the prospects and challenges in infrared photodetectors is presented.

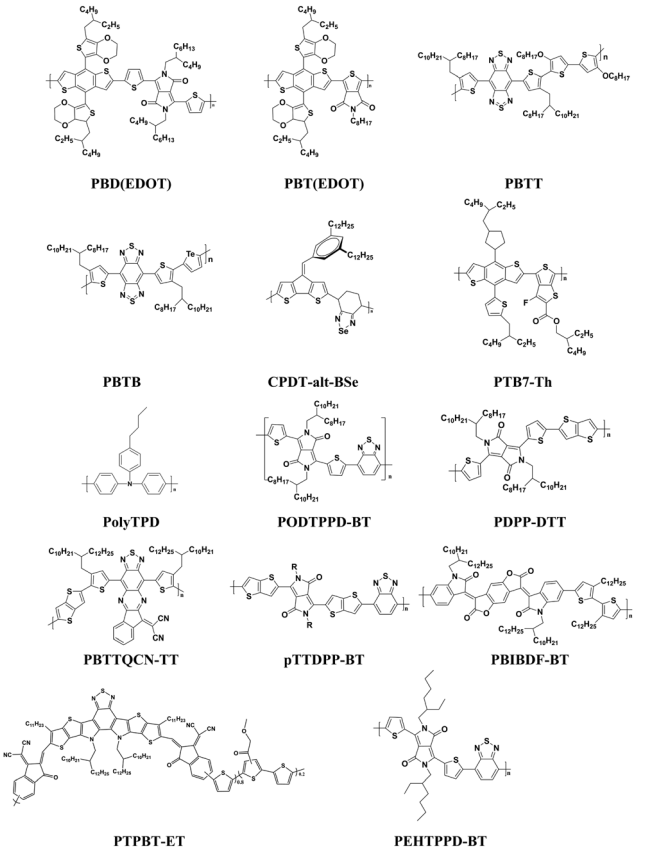

Scheme 1 Infrared photopolymers and their molecular structures.

2. Polymer-based photodiode

Organic photodetectors can realize the conversion of electromagnetic signals and photocurrent signals, so they are widely used in digital imaging, surveillance, environmental monitoring and optical communication. Compared with inorganic devices of the same type, organic photodiodes with the sandwich device structure shown in Fig. 1a can achieve weak signal detection and fast time response. Simultaneously with large-area detection capability, rich material selectivity, and low-cost

Liqiang Li

Liqiang Li is a professor at the Institute of Molecular Aggregation Sciences, Tianjin University. He received his Bachelor's degree (2002) and Master's degree (2005) from Nankai University. He obtained his doctor degree of physical chemistry in Institute of Chemistry, Chinese Academy of Sciences. Then, he worked as a postdoctoral scholar in Institute of Physics, Muenster University, Germany. In 2014, he joined Suzhou Institute of Nano-tech and Nano-bionics, Chinese Academy of Sciences in May, 2014. In 2018, he moved to Tianjin University. His research activities concentrate on assembly, property and electronic applications of molecular materials.

Wenping Hu

Wenping Hu is a professor of School of Science, Tianjin University, China. He received his PhD degree from Institute of Chemistry, Chinese Academy of Sciences in 1999 under the supervision of Prof. Daoben Zhu and Prof. Yunqi Liu. Then, he joined Osaka University and Stuttgart University as a research fellow of Japan Society for the Promotion of Sciences and Alexander von Humboldt, respectively. In 2003 he worked at Nippon Telephone and Telegraph, and then joined in ICCAS again as a full professor. Now, he is the vice president of the Tianjin University. His research interests focus on organic optoelectronics.

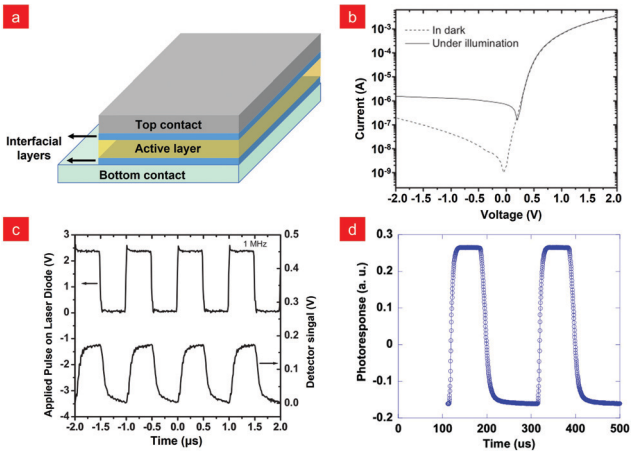

Fig. 1 (a) A schematic illustration of the typical geometries of OPDIs. (b) *I*–*V* characteristics of the PD in the dark and under 850 nm monochromatic illumination. (c) Transient response of a PD under 1 MHz modulated 850 nm monochromatic illumination. Reproduced with permission from ref. 29. Copyright 2007 Wiley-VCH. (d) Photoresponse of the OPDs to a 100 μs laser pulse at 852 nm with an incident power density of 10 mW cm^{-2}. Reproduced with permission from ref. 48. Copyright 2020 American Chemical Society.

fabrication on flexible substrates, they have been extensively studied and explored.[2,8,21,29–31] The organic photosensitive layers play an important role in absorbing photon energy to generate photogenerated excitons under illumination, and offer an platform for separating the electron–hole pairs and collecting the charge carriers by the electrode under a reverse bias.[22] Therefore, the photosensitive layers, such as pure polymer, polymer/inorganic hybrid and doped hybrid, will be described in detail in the following sub-sections.

2.1 Polymer active layer photodiode

Polymer photodetectors generally use bulk heterojunction (BHJ) structures to achieve efficient photon absorption and charge separation, in which polymer semiconductors are served as electron donors, and C_{60} or its functionalized derivatives are selected as electron acceptors.[32,33] In addition, infrared detection requires polymer semiconductors to possess the properties of low band gap, high fluidity, and solution processability, which has been limited by their difficult synthetic design.[11,22,23,34–38] In 2007, the Yang and co-workers research group designed and synthesized a new type of ester-modified low-bandgap (1.3 eV) polymer polythieno[3,4-*b*]thiophene (PTT).[29] The presence of the electron-withdrawing ester group in the polymer could stabilize the electron-rich thiophene and reduce its highest occupied molecular orbital (HOMO) energy level to match the (6,6)-phenyl C_{61}-butyric acid methyl ester (PCBM), and then the prepared photodiode could realize the effective detection of near-infrared light as shown in Fig. 1b with the rise and fall times both around 100 ns (Fig. 1c) thanks to the slow and dispersive transport of holes in the polymer PTT.[39] Besides traditional fullerene derivatives, researchers were also actively developing non-fullerene electron acceptors to obtain high-performance photodetectors[40–42] due to their advantages of adjustable optical band gap, strong absorption characteristics in the near-infrared region, and good charge transport capabilities.[43–47] For example, Cao and co-workers reported the fabrication of a highly sensitive visible-near infrared (NIR) photodetector based on wide-bandgap polymers as electron donors and non-fullerene small molecules as electron donors.[48] Fig. 1d demonstrated the measurement of the transient photocurrent of a device with a fast rise time of 12 μs and a fall time of 14 μs using an 852 nm pulsed laser.

However, the bulk heterojunction (BHJ) structure will make the transfer and injection of charges more difficult, making the polymer photodetector produce high dark current density when negatively biased, thus limiting its detection ability.[2,49,50] To solve this issue, Liang and co-workers proposed a new method to reduce its dark current.[51] Using modified 3,4-ethylenedioxythiophene (EDOT) as a conjugated side chain, they functionalized the main chain of the semiconducting polymer to synthesize molecules as shown in Scheme 1, achieving a two-level reduction in dark current density (Fig. 2a and b). This method is applicable to various polymer semiconductors and provides a feasible synthesis strategy for constructing polymers for high-performance photodetectors. Generally speaking, in the preparation of devices, most of the vacuum deposited metal is used as the upper electrode, but the doping of the organic active layer will inevitably occur, leading to high dark current.[51–53] In order to avoid the generation of dark current, Zhou and co-workers used transfer-printed conducting polymer (tp-CP) as the upper electrodes as shown in Fig. 2c.[54] With the method, the photodetector produced a dark current that was more than two orders of magnitude lower than that of a device using a vacuum deposition electrode. At the same time, due to the transmittance of the top tp-CP electrode similar to ITO, the double-sided response of the NIR photodetector to the incident light from the bottom or top was realized (Fig. 2d). In addition to using the above methods to limit the dark current for near-infrared detectors, molecular engineering can also be used to reduce the optical band gap to enhance the photon detection capability.[55] In 2020, Huang and co-workers designed and synthesized two kinds of conjugated polymers poly(benzobisthiadiazolebithiophene-tellurophene) (PBTT) and poly(benzobisthiadiazolebithiophene-4,4′-dioctyloxy-[2,2′bithiophene]) (PBTB) with an ultra-low band gap (0.8 eV), which showed a wide range and excellent light response to visible and infrared light. Moreover, based on the longer exciton lifetime, favourable film morphology and molecular orientation of PBTB, infrared response and image sensing on flexible OPD have been realized, showing excellent spatial light intensity detection capabilities (Fig. 2e).[56]

2.2 Organic/inorganic hybrid photodiode

Although the development of infrared photodiodes has long been limited by low responsivity and high dark current, researchers have continuously developed new methods for not only optimized device structures but also new molecular design strategies to improve the performance of photodetectors.[52,57–59] Thereinto, organic/inorganic hybrid photodiodes offer an effective approach to realize high-performance photodetectors, which, to a certain extent, could release the burden of a series of complex molecular

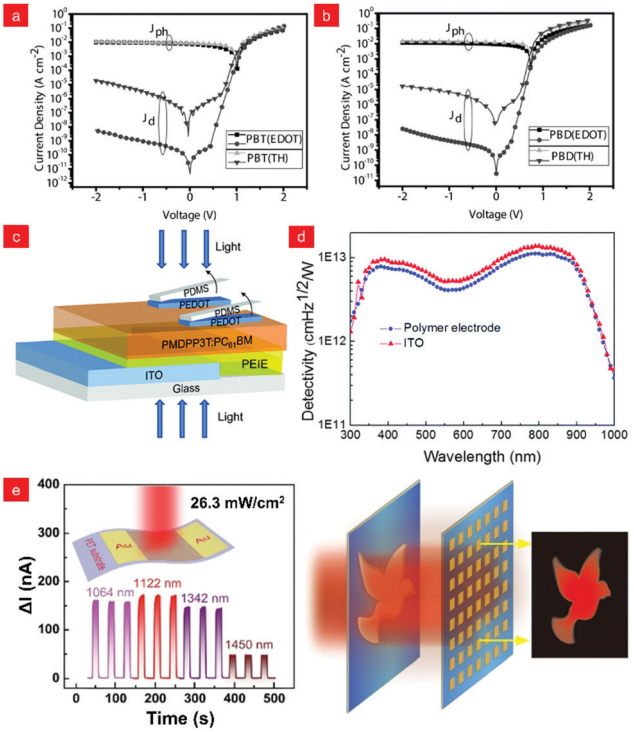

Fig. 2 J–V characteristics of (a) PBT(EDOT), PBT(TH) and (b) PBD(EDOT), PBD(TH) based photodetectors in the dark and under AM 1.5 G (100 mW cm^{-2}) illumination. Reproduced with permission from ref. 51. Copyright 2015 Wiley-VCH. (c) Device structure of IR OPDIs with transfer-printed contacts. (d) The detectivity of OPD *versus* the wavelength. The blue line is the detectivity of light incidence from the poly(3,4-ethylenedioxythiophene) : poly(styrenesulfo nate) (PEDOT : PSS) polymer top electrode and the red line is the detectivity of light incidence from the ITO bottom electrode. Reproduced with permission from ref. 54. Copyright 2016 Royal Society of Chemistry. (e) Schematic diagram of the device configuration of the flexible PD, and the photoresponse current at different wavelengths at 8 V and its image sensing. Reproduced with permission from ref. 56. Copyright 2020 American Chemical Society.

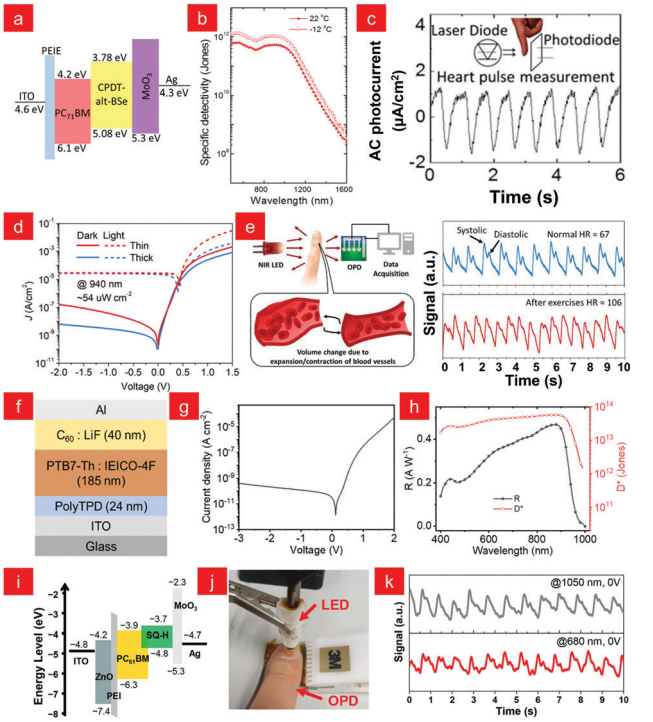

Fig. 3 (a) Energy diagram of the NIR photodiode. (b) Spectral dependence of the detectivity under different operating temperature at zero bias. (c) Photocurrent signals tracking a person's heart rate. Inset: Schematic diagram of the heart rate measurement. Reproduced with permission from ref. 66. Copyright 2016 American Chemical Society. (d) J–V curves of the OPDs in the dark and under illumination of NIR. (e) The working principle of NIR photoplethysmography and the pulsed signals measured from OPD before and after exercise. Reproduced with permission from ref. 11. Copyright 2019 Wiley-VCH. (f) Device structure, (g) dark J–V curve, (h) responsivity (R) and shot noise-limited specific detectivity (D^*) of the OPDI. Reproduced with permission from ref. 67. Copyright 2021 American Chemical Society. (i) Schematic device architecture and (j) the photoplethysmogram sensor demonstration of the SQ-H : PC$_{61}$BM blend-based OPDs. (k) Pulse signal measured from the OPD under 1050 and 680 nm LED illumination through the fingertip. Reproduced with permission from ref. 68. Copyright 2021 Wiley-VCH.

designs of polymers. As discussed in the following sub-sections, we will highlight two kinds of methods, such as interlayer mixed photodiode and hybrid photodiode.

2.2.1 Interlayer mixed photodiode. Inorganic materials have superior photosensitivity and charge transport capabilities,[60–62] while polymer materials have the potential for solution processability and the development of flexible devices. The combination of organic and inorganic is expected to achieve efficient exciton separation and charge transport processes.[63–65] In 2017, Ng and co-workers fabricated a NIR photodiode, which used the polymer CPDT-*alt*-BSe as the active layer and the inorganic material MoO_3 as the electron blocking layer with the energy levels of the different layers shown in Fig. 3a. From Fig. 3b, it can be seen that for infrared light, OPD had a detection rate as high as 10^{12} Jones, while the temperature dependence was small, and the application example of NIR photodiode detection of a fingertip arterial pulse is shown in Fig. 3c.[66] In 2019, Nguyen and co-workers demonstrated a near-infrared organic photodetector based on the ultra-narrow band gap non-fullerene acceptor CO1-4Cl. The detector used ZnO and MoO_3 as the hole/electron blocking layer, which effectively blocked the charge injection of the electrode into the donor polymer PTB7-Th, and realized sensitive sensing capability to 940 nm infrared light as shown in Fig. 3d. Moreover, the detection of human heart rate was realized by using the simulation diagram as shown in Fig. 3e.[11]

In 2021, Heremans and co-workers proposed a novel device stack as shown in Fig. 3f to fabricate low dark current infrared photodetectors. Their innovative use of crosslinked poly(*N*,*N*′-bis-4-butylphenyl-*N*,*N*′-bisphenyl)benzidine (PolyTPD) as an electron blocking layer provided effective blocking of electron injection and good device repeatability under reverse bias, achieving an ultra-low dark current density of 0.2 nA cm^{-2} (Fig. 3g) and a specific detection rate (D^*) of over 10^{13} Jones (Fig. 3g and h).[67] Würthner and co-workers demonstrated an organic photodiode with high sensitivity to short-wave infrared (SWIR, $\lambda > 1000$ nm) based on a dicyanovinyl functionalized squaraine dye (SQ-H) donor material. Using polyethyleneimine (PEI) as the charge blocking layer in the device framework, the

energy levels of different layers of the device are shown in Fig. 3i. The device constructed on the flexible substrate can realize the application of photoplethysmography for heart rate monitoring (Fig. 3j), and as a result, clear and periodic systolic and diastolic signals could be extracted with this photodetector for both wavelengths under ambient conditions (Fig. 3j and k).[68]

2.2.2 Hybrid photodiode. In the large-area fabrication of infrared photodetectors, the processing of organic semiconductors is obviously superior to the methods of epitaxial growth of inorganic semiconductors, so OPTs have more technological advantages. However, with small molecules and low-bandgap polymers, it is difficult to achieve sensitivity to infrared light with wavelengths greater than 1 μm.[29,69,70] The researchers turned their attention to hybrid photodiodes for high-performance long-wavelength detection.

For example, organic electrical detectors of hybrid quantum dots (QDS) have a more sensitive response and detection to infrared light.[71,72] Hayden and co-workers fabricated organic/inorganic hybrid photodiodes using a ternary mixture of PbS-QDs, PCBM, and poly(3-hexylthiophene) (P3HT) to form a heterostructure for photoresponsiveness. The sensor can also capture near-infrared images of insects.[63] In addition, nanowire (NW) PDs with an Ultraviolet (UV) to NIR response have potential applications in optical communication and interconnection in nanophotonic circuits, but their superior performance over a broad spectral range is required for practical applications.[73–75] To this end, Je and co-workers developed a high-performance stretchable UV-vis-NIR NWPD.[76] They adopted the common near-infrared sensitizer PbS and applied the direct writing technique shown in Fig. 4a to realize the PbS QD-P3HT hybrid NWPD. The stretchable UV-vis-NIR NWPD showed a nearly identical photoresponse under extreme (up to 100%) and repeated (up to 100 cycles) stretching conditions (Fig. 4b). This work applied the direct writing method of organic/inorganic hybrid nanowires to stretchable PD arrays, providing a new strategy for high-performance stretchable/flexible electronics.

Both solution-processable conjugated polymers and perovskite semiconductor materials possess unique optoelectronic properties. The discrete perovskite PDs are typically sensitive in the visible wavelength range, while the discrete polymer PDs exhibit a broadband photoresponse in the NIR wavelength range.[77–79] Visible-blind NIR photodetection with these broadband PDs requires the use of external bandpass filters or specially designed photonic structures for photodetection in a well-defined wavelength range.[80] But this will increase the extra cost, weaken the photosensitive performance, and also greatly increase the difficulty of applying them to flexible sensors. In 2021, Lan and co-workers designed a hybrid PD using a halide perovskite ($CH_3NH_3PbI_3$)/polymer hybrid heterojunction photoactive layer in the structure to achieve tunable detection visible-blind NIR by controlling the accumulation of space charges at the interface.[81] Among them, perovskite as a hole transport layer completely absorbed visible light and realized NIR bandpass, which demonstrated that PDs had narrow-band photodetection in the near-infrared wavelength range (Fig. 4c and d).

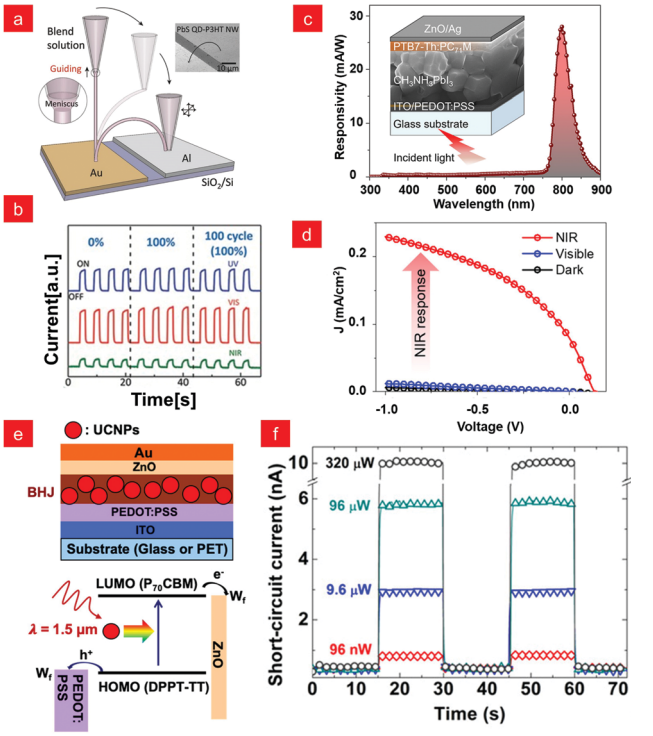

Fig. 4 (a) Directly written PbS QD-P3HT hybrid NW arches and (b) their stable photoresponse to different wavelengths under multiple stretching cycles. Reproduced with permission from ref. 76. Copyright 2015 Wiley-VCH. (c) Cross-sectional views, responsivity spectra and (d) optoelectronic properties of hybrid PDs with heterojunction photoactive layers. Reproduced with permission from ref. 81. Copyright 2021, American Chemical Society. (e) Schematic diagram of the hybrid BHJ/UCNP photodetector device architecture, schematic diagram of the upconversion working principle, and (f) time-dependent short-circuit currents under laser irradiation with a λ = 1.5 μm at different laser powers. Reproduced with permission from ref. 87. Copyright 2019 American Chemical Society.

Although the above works have improved the performance of photodetectors through processes, structures, *etc.*, the use of highly toxic heavy metal elements not only increased the production cost, but also caused serious ecological problems.[76,81,82] Therefore, it is also a current research hotspot to seek eco-friendly infrared photodetector strategies, such as two-dimensional materials such as graphene and colloidal quantum dots.[83–86] In 2019, Chen and co-workers demonstrated a high-performance, heavy-metal-free flexible photodetector sensitive to λ = 1.5 μm infrared light through a two-terminal structure (Fig. 4e). The photodetector design strategy utilized a solution-processable conjugated polymer/small molecule bulk heterojunction as the host and Er^{3+}-doped upconversion nanoparticles as the guest. The response mechanism is shown in Fig. 4e, where $NaYF_4:Er^{3+}$ upconversion nanoparticles (UCNPs) could efficiently upconvert λ = 1.5 μm photons to visible photons, and then transfer the energy to the organic BHJ host that generates the photocurrent. As shown in Fig. 4f, the BHJ/UCNP photodetector exhibited a good photoresponse, fast operation speed, and high reproducibility, opening up bright opportunities for next-generation low-cost and high-performance SWIR photodetectors.[87]

3. Polymer-based phototransistors

The promising potential of organic photodiodes for infrared detection has been reviewed previously, and compared with organic photodiodes, organic phototransistors (OPTs), as a three-terminal device (Fig. 5a), combine the signal amplification function of a transistor and the photodetection function of a single photodiode device, which can effectively control the channel carriers, the electric field distribution, and then enhance the photocurrent. Organic phototransistors can be fabricated at low temperatures, are more cost-effective, and can be integrated into optoelectronic logic circuits, all of which have contributed to their rapid development.[88–91] On the basis of organic phototransistors, both the active layers and the dielectric layers could affect the generation, separation, transmission of photogenerated excitons, and the trap state of the interface.[28] In the next sub-sections, we will further clarify the role of active layers and dielectric layers in modulating the performance of the devices.

3.1. Phototransistors of pure polymer semiconductors

The electrical properties of polymer semiconductors can be enhanced by the logical design of their structures (*i.e.*, polymer backbone and substituted alkyl side chains),[22] and ultrathin, lightweight, flexible, and bendable devices can be achieved through device fabrication processes, and these properties make it attractive as a favourable candidate for future photodetectors.[92–95]

Usually, charge trap sites are the main factors affecting their performance, and minority carrier trap sites assist the photomultiplier (PM) mechanism of semiconductors to improve the response and gain of photodetectors. Furthermore, the introduction of majority carrier trap sites can effectively reduce the dark current, thereby improving the detection performance.[2,97–100] On this basis, Shou and co-workers proposed a spatially separated hole/electron double trap mode for phototransistors, whose structure is shown in Fig. 5b.[96] They used metallic Ag nanoparticles and $PC_{61}BM$ as trapping sites for holes/electrons, respectively, and achieved spatial separation with the aid of a polymethyl methacrylate (PMMA) layer, resulting in low-noise currents and high photoresponsivity (5.26×10^3 A W^{-1}), exhibiting ultra-high detection rates ($D^*_{1/f} = 1.88 \times 10^{15}$ D$^*_{1/f}$ = 1.88×10^{15} Jones; $D^*_{shot} = 8.21 \times 10^{16}$ D$^*_{shot}$ = 8.21×10^{16} Jones). They also used confocal microscopy to scan micro-photocurrents to study the difference between two-terminal and three-terminal devices. In two-terminal devices, the carriers are uniformly distributed throughout the film; while in three-terminal devices, due to the large potential difference between gate and drain, charge separation becomes easier and higher photocurrent is obtained (Fig. 5e). Besides the above works, other studies on PM deserve attention. The narrowband of PM type photodetectors was prepared with thick active layers of P3HT : PCBM or P3HT : PTB7-Th : PCBM, and the narrowband spectral response of PM type photodetectors can be realized from the red to near infrared light range.[101,102] The spectral response range of PM-OPD can be extended to the near-infrared range based on narrow-bandgap non-fullerene materials as acceptors or by adopting a ternary strategy or a bilayer scheme.[103–106] These studies also provide new design strategies for photodetector research.

For phototransistors, in addition to having field effect characteristics and sufficiently large carrier mobility, the semiconductor channel layer should also be sensitive enough to infrared light. Conjugated polymers can achieve the above functions through pre-designed logic, showing unique advantages.[107–109] In 2020, Park and co-workers synthesized the conjugated polymer poly[{2,5-bis-(2-octyldodecyl)-3,6-bis-(thien-2yl)-pyrrolo[3,4-*c*]pyrrole-1,4-diyl}-*co*-{2,2′-(2,1,3-benzothiadiazole)5,5′-diyl}] (PODTPPD-BT) and used it as a near-infrared sensing channel layer (SCL) to fabricate a phototransistor with the structure shown in Fig. 6a. Moreover, a flexible near-infrared sensor with an effective

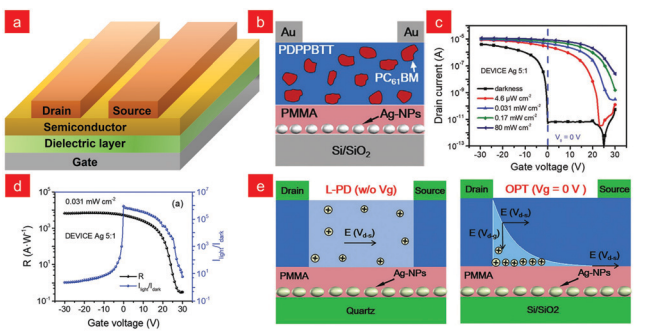

Fig. 5 (a) A schematic illustration of the typical geometries of OPTs. (b) Device structure of dual trap OPT. (c) Transfer characteristic curves of dual trap OPT without illumination and different illumination intensities at 820 nm. (d) Responsivity of dual trap OPT and I_{light}/I_{dark} dependence on a gate voltage. (e) Working model of OPDIs and OPTs. Reproduced with permission from ref. 96. Copyright 2021 Wiley-VCH.

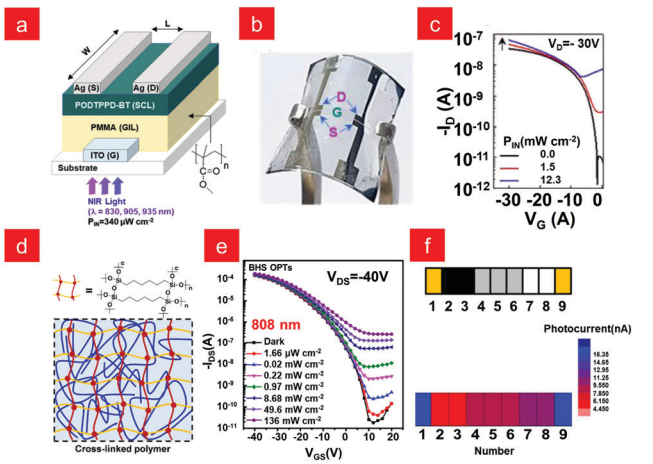

Fig. 6 (a) Device structure of the organic phototransistor (OPTR) with the PODTPPDBT sensing channel layer (SCL). (b) Photographs for the bent flexible OPTR. (c) Transfer curves according to the incident light intensity (P_{IN}) at λ = 905 nm. Reproduced with permission from ref. 110. Copyright 2020 Wiley-VCH. (d) Composition of the conducting channel in the BHS phototransistor. (e) Photoresponse characteristics of OPTs based on a PDPP-DTT polymer. (f) Photocurrent maps of OPTs under different shades of gray. Reproduced with permission from ref. 113. Copyright 2020 Elsevier.

response to λ = 905 nm was realized, showing its potential in the field of wearable electronics (Fig. 6b and c).[110] Generally, narrow-bandgap materials are one of the indispensable conditions for infrared light detection, but the low mobility and large dark current caused by narrow-bandgap polymers also limit the detection performance of infrared light.[5,6,80,111,112] In order to solve this problem, Liu and co-workers designed a polymer phototransistor with a bilayer heterostructure (BHS),[113] which could ensure efficient exciton separation and fast carrier transport. BHS selected cross-linked poly(*N*-alkyl diketo-pyrrolo-pyrrole dithienylthieno [3,2-*b*]thiophene) (PDPP-DTT) as the carrier transport layer, and its cross-linked structure is shown in Fig. 6d, using PDPP-DTT and $PC_{61}BM$ as the photosensitive layer. The device with the above structure had a high response to 808 nm light (Fig. 6e), while applying indanone-condensed thiadiazolo[3,4-*g*] quinoxaline-based polymer (PBTTQCN-TT) as the NIR light absorber, the phototransistors had a good response to 808 nm, 1064 nm, and 1550 nm NIR light, solving the difficult application of low-bandgap polymers in phototransistors. Based on the above methods, they also prepared flexible BHS OPTs with stable performance, which can realize the recognition of a barcode with different gray levels (Fig. 6f). This solution-processable BHS strategy has outstanding potential to develop flexible polymer phototransistors from NIR-I to NIR-II windows.

The research on phototransistors is mostly based on ultraviolet and visible light research, while the infrared light detection requires polymers with high mobility and a sufficiently narrow band gap,[37,38,114,115] so the BHJ structure is selected to expand the absorption spectrum[116–118] and improve the photoconductive gain of near-infrared light, however polymer blending in this structure can lead to phase stability problems.[119] In organic semiconductors, the exploration and development of conjugated polymers provides many polymer semiconductors with narrow band gaps and high mobility, which also provides new opportunities for single-component OPTs.[120,121] However, as mentioned above, most of the research on OPTs is p-type semiconductors, and there is a lack of attention to n-type and bipolar semiconductors.[122,123] In 2017, Kim and co-workers synthesized a polymer poly(3-(5(benzo[*c*][1,2,5]thiadiazol-4-yl)thieno [3,2-*b*]thiophen-2-yl)2,5-bis(2-octyldodecyl)-6-(thieno[3,2-*b*]thiophen-2-yl)pyrrolo[3,4-*c*]pyrrole-1,4(2*H*,5*H*)-dione) (pTTDPP-BT) with dual acceptor molecules. The constructed transistor device showed bipolar charge transport behaviour, and the annealed optimized phototransistor showed a photoresponse over a wide range of wavelengths (405–850 nm) (Fig. 7a).[111] In 2018, Wang and co-workers also synthesized bipolar donor–acceptor (D–A) conjugated polymers PBIBDF-BT based on a bis(2-oxoindolin-3-ylidene)-benzodifuran-dione (BIBDF) acceptor, and successfully prepared flexible n-type NIR OPTs capable of low-voltage operation using the AlO_x/SAM of n-octadecyl phosphonic acid (ODPA-SAMs) as a dielectric layer, and the device exhibited good photoresponsivity and mechanical flexibility (Fig. 7b).[124]

3.2. Organic/inorganic hybrid semiconductor phototransistors

Despite the many advantages of polymer semiconductors, polymer phototransistors generally exhibit moderate

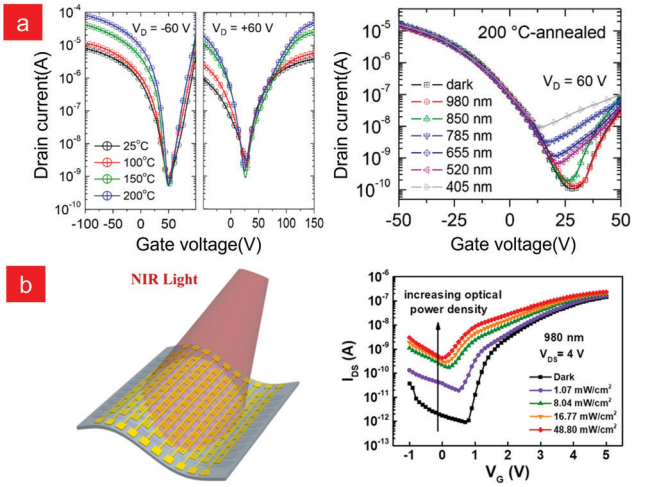

Fig. 7 (a) Performance of photoresponsive transistors based on double-acceptor-containing low-bandgap polymers. Reproduced with permission from ref. 111. Copyright 2017 American Chemical Society. (b) Flexible, low-voltage and n-type infrared organic phototransistors and photoresponsive properties. Reproduced with permission from ref. 124. Copyright 2018 American Chemical Society.

performance because the collection of photogenerated carriers is limited by the low carrier mobility of polymer semiconductors.[7] Therefore, a heterojunction phototransistor composed of mixed photosensitive and carrier transport channels is developed, which can simultaneously achieve a high near-infrared response and fast charge recycling.[125–127]

Organometallic halide perovskite materials have attracted much attention due to their excellent optoelectronic properties.[128,129] In 2017, Xie and co-workers constructed a ternary vertical multi-heterojunction phototransistor, with $CH_3NH_3PbI_{3-x}Cl_x$ as the photoactive layer, absorbing infrared light to generate electron–hole pairs; poly(3-hexylthiophene) (P3HT) as the hole transport layer to separate electrons and holes; the graphene layer provided a fast charge transport channel, enabling highly sensitive infrared light detection at a low voltage of 0.1 V(Fig. 8a).[130] Subsequently, Kim and co-workers decoupled and independently optimized the charge generation and transport processes, achieving better performance than commercial germanium phototransistors.[131] They improved the organic BHJ layer by exploiting the feature that camphor can increase the carrier lifetime, and at the same time using indium zinc oxide as the transport layer for fast charge transport, achieving a high specific detection rate over a wide spectral range ($500 < \lambda < 1300$ nm, 5×10^{12} Jones), expanding a new avenue for realizing solution-processable infrared phototransistors (Fig. 8b). In 2021, Li and co-workers based on indium oxide (In_2O_3) and n-type polymerizing small-molecular acceptors (PSMA) polymer semiconductor of poly{5,5′-bis[3,5-bis(thienyl) phenyl]-2,2′-bithiophene-3ethylesterthiophene]} (PTPBT-ET) successfully prepared air-stable high-performance infrared phototransistors (Fig. 8c),[132] in which In_2O_3 thin-film transistors (TFTs) could provide high electrical performance and uniformity, and PTPBT-ET as a new PSMA enabled large photocurrents and long-term

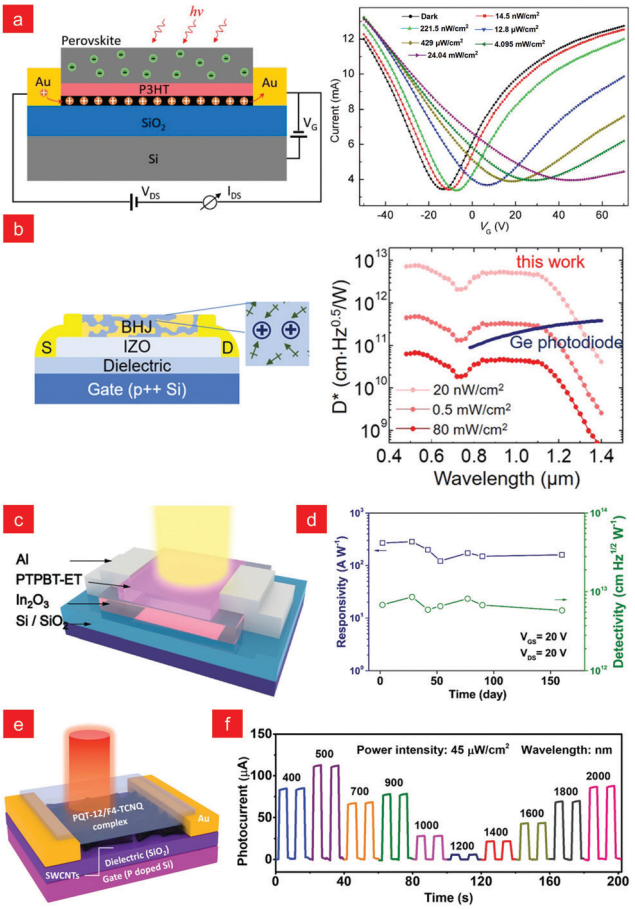

Fig. 8 (a) Structure diagram and photoresponse current of a perovskite/graphene vertical heterojunction phototransistor with a P3HT hole transport layer. Reproduced with permission from ref. 130. Copyright 2017 American Chemical Society. (b) Phototransistor structure, photoresponse and detectivity with indium zinc oxide (IZO) as the electron transport layer. Reproduced with permission from ref. 131. Copyright 2019 American Chemical Society. (c) The schematic illustration of the In_2O_3/PTPBTET hybrid phototransistor structure. (d) The responsivity and detectivity as a function of different days from fabrication. Reproduced with permission from ref. 132. Copyright 2021 Wiley-VCH. (e) Schematic diagram of the PQT-12/F4-TCNQ based organic IR phototransistor. (f) The photocurrent of the phototransistor at different wavelengths. Reproduced with permission from ref. 138. Copyright 2021 Wiley-VCH.

stability.[133] The device constructed by the above strategy successfully achieved a high specific detection rate of 1.2×10^{13} Jones at 810 nm NIR light and a long-term stable performance of more than 160 days (Fig. 8d).

Due to the wide band gap of most organic semiconductors, only very few organic phototransistors can realize the response to infrared light with $\lambda > 1500$ nm,[80,122,134–136] which greatly limits the application in long-wavelength light.[22,137] Huang and co-workers fabricated an organic phototransistor with a ternary semiconductor of semiconducting single-walled carbon nanotubes (SWCNTs) and organic donor/acceptor complexes with the structure shown in Fig. 8e, which enabled broadband photodetection (400–2600 nm) (Fig. 8f). Among them, compound semiconductors achieved ultra-broad spectral absorption due to their ultra-low electronic transition energy (0.4 eV) as photoactive layers, and semiconductor SWCNTs provided charge transport capability with a high on/off ratio, low dark current, and wide gate tuning range. These studies provide new guidelines for fabricating organic infrared phototransistors capable of operating at room temperature.[138]

3.3. Phototransistors with polymer dielectric layers

As mentioned above, most infrared organic phototransistors use organic semiconductor layers as infrared sensing layers, which requires these materials not only to have good transistor characteristics, but also to be sensitive to infrared light.[117,123,139,140] In order to further promote the development of infrared phototransistors, a new type of organic phototransistor architecture with a kind of gate sensing layer was designed.

In 2018, Han and co-workers proposed the transistor architecture shown in Fig. 9a, in which a conjugated polymer without field-effect properties was placed between the gate and the dielectric layer as the NIR sensing layer, called the NIR Gate Sensing Layer (GSL). They used the conjugated polymer poly [{2,5-bis-(2-ethylhexyl)-3,6-bis-(thien-2-yl)-pyrrolo[3,4-*c*]pyrrole-1,4-diyl}co-{2,2′-(2,1,3-benzothiadiazole)]-5,5′-diyl}] (PEHTTPD-BT) as the gate sensing layer to realize stable detection of infrared light (Fig. 9b).[141] In fact, for the infrared absorption of organic materials, it can also be achieved by covalent bonding and doping to narrow the band gap.[142,143] Covalent bonding can achieve the infrared absorption range of organic materials below $\lambda = 1800$ nm,[144–146] while the doping method can provide extremely high shifted infrared absorption up to $\lambda = 2000$ nm.[147–150] In 2021, Lee and co-workers realized the doping of polytriarylamine, poly[*N*,*N*′-bis(4-butylphenyl)-*N*,*N*′-bis(phenyl) benzidine] (PolyTPD) with

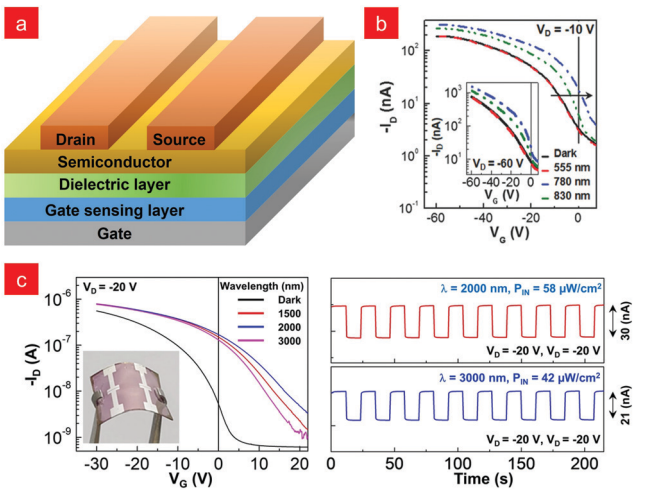

Fig. 9 (a) Organic phototransistor device structure with a gate sensing layer (GSL). (b) Transfer at $V_D = -10$ V (inset: at $V_D = -60$ V) curves for the Organic Phototransistor with Gate Sensing Layer (GSL) in the dark and under illumination ($P_{IN} = 437.5$ μW cm^{-2}). Reproduced with permission from ref. 141. Copyright 2018 Wiley-VCH. (c) Transfer curves and photomodulation current changes of flexible SWIR-OPTR with PolyTPD : BCF GSL under short-wave infrared light irradiation. Reproduced with permission from ref. 151. Copyright 2021 Springer Nature.

tris(pentafluorophenyl)borane (BCF), and well-controlled SWIR absorption (up to λ = ~3200 nm) was obtained. An organic phototransistor (OPTR) with BCF-doped PolyTPD film as the gate sensing layer (GSL) could detect SWIR light, and its flexible devices had high sensing stability (Fig. 9b), and exhibited a good sensing stability upon on/off modulations of the incident SWIR light (P_{IN} = 58 μW cm^{-2} at λ = 2000 nm and 42 μW cm^{-2} at λ = 3000 nm) (Fig. 9c).[151]

4. Challenges and perspectives

In the past, polymer-based photodetectors have made great strides in the sensitive detection of broadband infrared light. Whether it is the proposal of new molecular design strategies or the construction of new device structures, they have vigorously promoted the development of infrared photodetectors and realized the integrated application of infrared photodetectors in infrared imaging, human health detection, *etc.* All of these demonstrate the application potential of polymer-based flexible detectors in electronic skin and flexible wearable devices. However, at this stage, it is difficult for polymer-based photodetectors to meet the needs of social development. In daily life, industry, military and other fields, more stable detectors with better performance are still needed to deal with applications in different scenarios. First, as one of the most important components of the device, polymer semiconductors play a leading role in the performance of the device, and the design and synthesis of polymer semiconductor materials with efficient infrared absorption and high carrier mobility should be the primary goal. Secondly, the large-area integration of the device is a prerequisite for its application, and it is also necessary for high-resolution infrared imaging. While solution processability is an advantage of polymers, the polymer's intolerance to high temperature industries and certain solvents limit the development of the process. The large-scale fabrication of devices still has technological deficiencies, and it is difficult to achieve successful fabrication of high-performance, large-scale devices, and the exploration of processes is still urgent. Finally, the development of polymer-based infrared photodetectors should ultimately serve the application. Most of the polymer semiconductors are extremely sensitive to external environments such as water and oxygen, and their stability is also an urgent problem to be solved. Especially for application scenarios under extreme conditions, the devices need to have better tolerance. For the many challenges faced by photodetectors, researchers are also making continuous efforts to realize the integration and practical application of the device.

Conflicts of interest

There are no conflicts to declare.

Acknowledgements

The authors are grateful to the National Key Research and Development Program of China (2021YFA0717900), the National Natural Science Foundation of China (62004138, 21573277, 51503221 and 21905199), the Beijing National Laboratory for Molecular Sciences (BNLMS202006) and the Haihe Laboratory of Sustainable Chemical Transformations for financial support.

References

1 S. O. Kelley, C. A. Mirkin, D. R. Walt, R. F. Ismagilov, M. Toner and E. H. Sargent, *Nat. Nanotechnol.*, 2014, **9**, 969–980.
2 K.-J. Baeg, M. Binda, D. Natali, M. Caironi and Y.-Y. Noh, *Adv. Mater.*, 2013, **25**, 4267–4295.
3 R. D. Jansen-van Vuuren, A. Armin, A. K. Pandey, P. L. Burn and P. Meredith, *Adv. Mater.*, 2016, **28**, 4766–4802.
4 L. Gao, K. Zeng, J. S. Guo, C. Ge, J. Du, Y. Zhao, C. Chen, H. Deng, Y. S. He, H. S. Song, G. D. Niu and J. Tang, *Nano Lett.*, 2016, **16**, 7446–7454.
5 N. Li, Z. J. Lan, L. F. Cai and F. R. Zhu, *J. Mater. Chem. C*, 2019, **7**, 3711–3729.
6 C. Liu, K. Wang, X. Gong and A. J. Heeger, *Chem. Soc. Rev.*, 2016, **45**, 4825–4846.
7 F. P. G. de Arquer, A. Armin, P. Meredith and E. H. Sargent, *Nat. Rev. Mater.*, 2017, **2**, 16100.
8 X. Liu, Y. Lin, Y. Liao, J. Wu and Y. Zheng, *J. Mater. Chem. C*, 2018, **6**, 3499–3513.
9 Y. Lei, N. Li, W.-K. E. Chan, B. S. Ong and F. Zhu, *Org. Electron.*, 2017, **48**, 12–18.
10 M. Zhu, S. Lv, Q. Wang, G. Zhang, H. Lu and L. Qiu, *Nanoscale*, 2016, **8**, 7738–7748.
11 J. F. Huang, J. Lee, J. Vollbrecht, V. V. Brus, A. L. Dixon, D. X. Cao, Z. Y. Zhu, Z. F. Du, H. B. Wang, K. Cho, G. C. Bazan and T. Q. Nguyen, *Adv. Mater.*, 2020, **32**, 1906027.
12 K. M. Xu, W. J. Zhou and Z. J. Ning, *Small*, 2020, **16**, 2003397.
13 W. Lei, J. Antoszewski and L. Faraone, *Appl. Phys. Rev.*, 2015, **2**, 041303.
14 A. Rogalski, J. Antoszewski and L. Faraone, *J. Appl. Phys.*, 2009, **105**, 091101.
15 S. Y. Zhu, H. S. Chu, G. Q. Lo, P. Bai and D. L. Kwong, *Appl. Phys. Lett.*, 2012, **100**, 061109.
16 K. Zang, D. K. Zhang, Y. J. Huo, X. C. Chen, C. Y. Lu, E. T. Fei, T. I. Kamins, X. Feng, Y. D. Huang and J. S. Harris, *Appl. Phys. Lett.*, 2015, **106**, 101111.
17 C. Yu, X. Li, B. Yang, S. Huang, X. Shao, Y. Zhang and H. Gong, *Infrared Phys. Technol.*, 2017, **85**, 74–80.
18 D. Z. Yang and D. G. Ma, *Adv. Opt. Mater.*, 2019, **7**, 1800522.
19 X. F. Wang, L. Lv, L. L. Li, Y. S. Chen, K. Zhang, H. R. Chen, H. L. Dong, J. S. Huang, G. Z. Shen, Z. Yang and H. Huang, *Adv. Funct. Mater.*, 2016, **26**, 6306–6315.
20 C. Xie and F. Yan, *Small*, 2017, **13**, 1701822.
21 B. Y. Zhang, M. T. Trinh, B. Fowler, M. Ball, Q. Z. Xu, F. Ng, M. L. Steigerwald, X. Y. Zhu, C. Nuckolls and Y. Zhong, *J. Am. Chem. Soc.*, 2016, **138**, 16426–16431.

22 C. Wang, X. T. Zhang and W. P. Hu, *Chem. Soc. Rev.*, 2020, **49**, 653–670.
23 O. Ostroverkhova, *Chem. Rev.*, 2016, **116**, 13279–13412.
24 C. Fuentes-Hernandez, W. F. Chou, T. M. Khan, L. Diniz, J. Lukens, F. A. Larrain, V. A. Rodriguez-Toro and B. Kippelen, *Science*, 2020, **370**, 698.
25 Y. H. Zhou, C. Fuentes-Hernandez, J. Shim, J. Meyer, A. J. Giordano, H. Li, P. Winget, T. Papadopoulos, H. Cheun, J. Kim, M. Fenoll, A. Dindar, W. Haske, E. Najafabadi, T. M. Khan, H. Sojoudi, S. Barlow, S. Graham, J. L. Bredas, S. R. Marder, A. Kahn and B. Kippelen, *Science*, 2012, **336**, 327–332.
26 P. Buechele, M. Richter, S. F. Tedde, G. J. Matt, G. N. Ankah, R. Fischer, M. Biele, W. Metzger, S. Lilliu, O. Bikondoa, J. E. Macdonald, C. J. Brabec, T. Kraus, U. Lemmer and O. Schmidt, *Nat. Photonics*, 2015, **9**, 843–848.
27 B. Lucas, T. Trigaud and C. J. P. I. Videlot-Ackermann, *Polym. Int.*, 2012, **61**, 374–389.
28 X. Huang, D. Ji, H. Fuchs, W. Hu and T. Li, *ChemPhotoChem*, 2020, **4**, 9–38.
29 Y. Yao, Y. Y. Liang, V. Shrotriya, S. Q. Xiao, L. P. Yu and Y. Yang, *Adv. Mater.*, 2007, **19**, 3979.
30 P. Peumans, V. Bulovic and S. R. Forrest, *Appl. Phys. Lett.*, 2000, **76**, 3855–3857.
31 D. Z. Yang and D. G. Ma, *J. Mater. Chem. C*, 2013, **1**, 2054–2060.
32 G. Yu, J. Gao, J. C. Hummelen, F. Wudl and A. J. Heeger, *Science*, 1995, **270**, 1789–1791.
33 P. Schilinsky, C. Waldauf and C. J. Brabec, *Appl. Phys. Lett.*, 2002, **81**, 3885–3887.
34 R. A. Janssen, J. C. Hummelen and N. S. Sariciftci, *MRS Bull.*, 2005, **30**, 33–36.
35 W. Deng, Y. Lv, X. Zhang, X. Fang, B. Lu, Z. Lu and J. Jie, *Mater. Today*, 2020, **40**, 82–90.
36 Y. Guo, C. Du, G. Yu, C.-A. Di, S. Jiang, H. Xi, J. Zheng, S. Yan, C. Yu, W. Hu and Y. Liu, *Adv. Funct. Mater.*, 2010, **20**, 1019–1024.
37 K. H. Hendriks, W. W. Li, M. M. Wienk and R. A. J. Janssen, *J. Am. Chem. Soc.*, 2014, **136**, 12130–12136.
38 C. S. Smithson, Y. L. Wu, T. Wigglesworth and S. P. Zhu, *Adv. Mater.*, 2015, **27**, 228–233.
39 N. Rappaport, O. Solomesch and N. Tessler, *J. Appl. Phys.*, 2006, **99**, 064507.
40 C. Q. Yan, S. Barlow, Z. H. Wang, H. Yan, A. K. Y. Jen, S. R. Marder and X. W. Zhan, *Nat. Rev. Mater.*, 2018, **3**, 18003.
41 Y. Z. Lin, Q. He, F. W. Zhao, L. J. Huo, J. Q. Mai, X. H. Lu, C. J. Su, T. F. Li, J. Y. Wang, J. S. Zhu, Y. M. Sun, C. R. Wang and X. W. Zhan, *J. Am. Chem. Soc.*, 2016, **138**, 2973–2976.
42 Y. Z. Lin and X. W. Zhan, *Mater. Horiz.*, 2014, **1**, 470–488.
43 Y. Z. Lin, J. Y. Wang, Z. G. Zhang, H. T. Bai, Y. F. Li, D. B. Zhu and X. W. Zhan, *Adv. Mater.*, 2015, **27**, 1170–1174.
44 Y. Z. Lin, F. W. Zhao, Q. He, L. J. Huo, Y. Wu, T. C. Parker, W. Ma, Y. M. Sun, C. R. Wang, D. B. Zhu, A. J. Heeger, S. R. Marder and X. W. Zhan, *J. Am. Chem. Soc.*, 2016, **138**, 4955–4961.
45 J. Y. Wang, J. X. Zhang, Y. Q. Xiao, T. Xiao, R. Y. Zhu, C. Q. Yan, Y. Q. Fu, G. H. Lu, X. H. Lu, S. R. Marder and X. W. Zhan, *J. Am. Chem. Soc.*, 2018, **140**, 9140–9147.
46 S. X. Dai, F. W. Zhao, Q. Q. Zhang, T. K. Lau, T. F. Li, K. Liu, Q. D. Ling, C. R. Wang, X. H. Lu, W. You and X. W. Zhan, *J. Am. Chem. Soc.*, 2017, **139**, 1336–1343.
47 B. Y. Jia, J. Wang, Y. Wu, M. Y. Zhang, Y. F. Jiang, Z. Tang, T. P. Russell and X. W. Zhan, *J. Am. Chem. Soc.*, 2019, **141**, 19023–19031.
48 G. H. Liu, T. F. Li, X. W. Zhan, H. B. Wu and Y. Cao, *ACS Appl. Mater. Interfaces*, 2020, **12**, 17769–17775.
49 Y. J. Xia, L. Wang, X. Y. Deng, D. Y. Li, X. H. Zhu and Y. Cao, *Appl. Phys. Lett.*, 2006, **89**, 081106.
50 M. Kaltenbrunner, M. S. White, E. D. Glowacki, T. Sekitani, T. Someya, N. S. Sariciftci and S. Bauer, *Nat. Commun.*, 2012, **3**, 770.
51 L. Z. Zhang, T. B. Yang, L. Shen, Y. J. Fang, L. Dang, N. J. Zhou, X. G. Guo, Z. R. Hong, Y. Yang, H. B. Wu, J. S. Huang and Y. Y. Liang, *Adv. Mater.*, 2015, **27**, 6496.
52 A. Pierre, I. Deckman, P. B. Lechene and A. C. Arias, *Adv. Mater.*, 2015, **27**, 6411.
53 R. S. Nowicki, *Gold Bull.*, 1982, **15**, 21–24.
54 S. X. Xiong, J. H. Tong, L. Mao, Z. F. Li, F. Qin, F. Y. Jiang, W. Meng, T. F. Liu, W. W. Li and Y. H. Zhou, *J. Mater. Chem. C*, 2016, **4**, 1414–1419.
55 G. Bhat, Q. Liu, M. Kielar, Y. Hamada, T. Michinobu, P. Sah, A. K. K. Kyaw, A. K. Pandey and P. Sonar, *ACS Appl. Mater. Interfaces*, 2021, **13**, 29866–29875.
56 L. Lv, W. Dang, X. X. Wu, H. Chen, T. Wang, L. Q. Qin, Z. X. Wei, K. Zhang, G. Z. Shen and H. Huang, *Macromolecules*, 2020, **53**, 10636–10643.
57 G. Simone, M. J. Dyson, S. C. J. Meskers, R. A. J. Janssen and G. H. Gelinck, *Adv. Funct. Mater.*, 2020, **30**, 1904205.
58 S. Yoon, J. Ha, J. Cho and D. S. Chung, *Adv. Opt. Mater.*, 2016, **4**, 1933–1938.
59 B. Xie, Z. Chen, L. Ying, F. Huang and Y. Cao, *InfoMat*, 2020, **2**, 57–91.
60 J.-S. Lee, M. V. Kovalenko, J. Huang, D. S. Chung and D. V. Talapin, *Nat. Nanotechnol.*, 2011, **6**, 348–352.
61 P. Dutta, M. Rathi, N. Zheng, Y. Gao, Y. Yao, J. Martinez, P. Ahrenkiel and V. Selvamanickam, *Appl. Phys. Lett.*, 2014, **105**, 092104.
62 X. Hu, J. Wu, M. Wu and J. Hu, *Nano Res.*, 2022, **15**, 805–817.
63 T. Rauch, M. Boberl, S. F. Tedde, J. Furst, M. V. Kovalenko, G. N. Hesser, U. Lemmer, W. Heiss and O. Hayden, *Nat. Photonics*, 2009, **3**, 332–336.
64 Z. Tang, Z. Ma, A. Sanchez-Diaz, S. Ullbrich, Y. Liu, B. Siegmund, A. Mischok, K. Leo, M. Campoy-Quiles, W. Li and K. Vandewal, *Adv. Mater.*, 2017, **29**, 1702184.
65 L. Shen, Y. Lin, C. Bao, Y. Bai, Y. Deng, M. Wang, T. Li, Y. Lu, A. Gruverman, W. Li and J. Huang, *Mater. Horiz.*, 2017, **4**, 242–248.
66 Z. H. Wu, W. C. Yao, A. E. London, J. D. Azoulay and T. N. Ng, *ACS Appl. Mater. Interfaces*, 2017, **9**, 1654–1660.

67 W. T. Yang, W. M. Qu, E. Georgitzikis, E. Simoen, J. Serron, J. Lee, I. Lieberman, D. Cheyns, P. Malinowski, J. Genoe, H. Z. Chen and P. Heremans, *ACS Appl. Mater. Interfaces*, 2021, **13**, 16766–16774.
68 J. H. Kim, A. Liess, M. Stolte, A. M. Krause, V. Stepanenko, C. W. Zhong, D. Bialas, F. C. Spano and F. Wurthner, *Adv. Mater.*, 2021, **33**, 2100582.
69 I. W. Hwang, C. Soci, D. Moses, Z. G. Zhu, D. Waller, R. Gaudiana, C. J. Brabec and A. J. Heeger, *Adv. Mater.*, 2007, **19**, 2307.
70 D. Natali, M. Sampietro, M. Arca, C. Denotti and F. A. Devillanova, *Synth. Met.*, 2003, **137**, 1489–1490.
71 L. Chu, A. Zrenner, G. Bohm and G. Abstreiter, *Appl. Phys. Lett.*, 1999, **75**, 3599–3601.
72 H. C. Liu, L. Li, M. Buchanan, Z. R. Wasilewski, G. J. Brown, F. Szmulowicz and S. M. Hegde, *J. Appl. Phys.*, 1998, **83**, 585–587.
73 Z. X. Wang, M. Safdar, C. Jiang and J. He, *Nano Lett.*, 2012, **12**, 4715–4721.
74 Z. Liu, T. Luo, B. Liang, G. Chen, G. Yu, X. M. Xie, D. Chen and G. Z. Shen, *Nano Res.*, 2013, **6**, 775–783.
75 G. Chen, B. Liang, X. Liu, Z. Liu, G. Yu, X. M. Xie, T. Luo, D. Chen, M. Q. Zhu, G. Z. Shen and Z. Y. Fan, *ACS Nano*, 2014, **8**, 787–796.
76 J. Yoo, S. Jeong, S. Kim and J. H. Je, *Adv. Mater.*, 2015, **27**, 1712.
77 Z. H. Xu, Y. G. Yu, S. Arya, I. A. Niaz, Y. M. Chen, Y. S. Lei, M. A. Miah, J. Y. Zhou, A. C. Zhang, L. J. Yan, S. Xu, K. Nomura and Y. H. Lo, *Nano Lett.*, 2020, **20**, 2144–2151.
78 N. Li, W. X. Lan, Y. S. Lau, L. F. Cai, A. A. Syed and F. R. Zhu, *J. Mater. Chem. C*, 2019, **7**, 9573–9580.
79 N. Li, Y. L. Lei, W. K. E. Chan and F. R. Zhu, *J. Mater. Chem. C*, 2019, **7**, 4808–4816.
80 N. Li, Z. J. Lan, Y. S. Lau, J. J. Xie, D. H. Zhao and F. R. Zhu, *Adv. Sci.*, 2020, **7**, 2000444.
81 Z. J. Lan, L. F. Cai, D. Luo and F. R. Zhu, *ACS Appl. Mater. Interfaces*, 2021, **13**, 981–988.
82 F. Li, Z. Qiu, S. Liu and H. Zhang, *ACS Appl. Nano Mater.*, 2019, **2**, 4974–4982.
83 X. T. Gan, R. J. Shiue, Y. D. Gao, I. Meric, T. F. Heinz, K. Shepard, J. Hone, S. Assefa and D. Englund, *Nat. Photonics*, 2013, **7**, 883–887.
84 Y. Xie, B. Zhang, S. X. Wang, D. Wang, A. Z. Wang, Z. Y. Wang, H. H. Yu, H. J. Zhang, Y. X. Chen, M. W. Zhao, B. B. Huang, L. M. Mei and J. Y. Wang, *Adv. Mater.*, 2017, **29**, 1605972.
85 N. Youngblood, C. Chen, S. J. Koester and M. Li, *Nat. Photonics*, 2015, **9**, 247–252.
86 G. Konstantatos, I. Howard, A. Fischer, S. Hoogland, J. Clifford, E. Klem, L. Levina and E. H. Sargent, *Nature*, 2006, **442**, 180–183.
87 H. Y. Xiang, Z. L. Hu, L. Billot, L. Aigouy, W. M. Zhang, I. McCulloch and Z. Y. Chen, *ACS Appl. Mater. Interfaces*, 2019, **11**, 42571–42579.
88 G. Horowitz, *Adv. Mater.*, 1998, **10**, 365–377.
89 B. Mukherjee, M. Mukherjee, K. Sim and S. Pyo, *J. Mater. Chem.*, 2011, **21**, 1931–1936.
90 B. Mukherjee, K. Sim, T. J. Shin, J. Lee, M. Mukherjee, M. Ree and S. Pyo, *J. Mater. Chem.*, 2012, **22**, 3192–3200.
91 X. Liu, E. K. Lee, D. Y. Kim, H. Yu and J. H. Oh, *ACS Appl. Mater. Interfaces*, 2016, **8**, 7291–7299.
92 J. G. Mei and Z. N. Bao, *Chem. Mater.*, 2014, **26**, 604–615.
93 J. G. Mei, D. H. Kim, A. L. Ayzner, M. F. Toney and Z. A. Bao, *J. Am. Chem. Soc.*, 2011, **133**, 20130–20133.
94 I. Meager, R. S. Ashraf, S. Rossbauer, H. Bronstein, J. E. Donaghey, J. Marshall, B. C. Schroeder, M. Heeney, T. D. Anthopoulos and I. McCulloch, *Macromolecules*, 2013, **46**, 5961–5967.
95 M. Q. He, J. F. Li, M. L. Sorensen, F. X. Zhang, R. R. Hancock, H. H. Fong, V. A. Pozdin, D. M. Smilgies and G. G. Malliaras, *J. Am. Chem. Soc.*, 2009, **131**, 11930–11938.
96 M. H. Shou, Q. L. Zhang, H. Li, S. C. Xiong, B. Y. Hu, J. D. Zhou, N. Zheng, Z. Q. Xie, L. Ying and L. L. Liu, *Adv. Opt. Mater.*, 2021, **9**, 2002031.
97 Y. J. Fang, F. W. Guo, Z. G. Xiao and J. S. Huang, *Adv. Opt. Mater.*, 2014, **2**, 348–353.
98 F. W. Guo, B. Yang, Y. B. Yuan, Z. G. Xiao, Q. F. Dong, Y. Bi and J. S. Huang, *Nat. Nanotechnol.*, 2012, **7**, 798–802.
99 L. L. Li, F. J. Zhang, J. Wang, Q. S. An, Q. Q. Sun, W. B. Wang, J. Zhang and F. Teng, *Sci. Rep.*, 2015, **5**, 9181.
100 L. L. Li, F. J. Zhang, W. B. Wang, Q. S. An, J. Wang, Q. Q. Sun and M. Zhang, *ACS Appl. Mater. Interfaces*, 2015, **7**, 5890–5897.
101 W. Wang, F. Zhang, M. Du, L. Li, M. Zhang, K. Wang, Y. Wang, B. Hu, Y. Fang and J. Huang, *Nano Lett.*, 2017, **17**, 1995–2002.
102 M. Liu, J. Wang, Z. Zhao, K. Yang, P. Durand, F. Ceugniet, G. Ulrich, L. Niu, Y. Ma, N. Leclerc, X. Ma, L. Shen and F. Zhang, *J. Phys. Chem. Lett.*, 2021, **12**, 2937–2943.
103 M. Liu, J. Wang, K. Yang, Z. Zhao, Z. Zhou, Y. Ma, L. Shen, X. Ma and F. Zhang, *J. Mater. Chem. C*, 2021, **9**, 6357–6364.
104 Z. Zhao, B. Liu, C. Xie, Y. Ma, J. Wang, M. Liu, K. Yang, Y. Xu, J. Zhang, W. Li, L. Shen and F. Zhang, *Sci. China: Chem.*, 2021, **64**, 1302–1309.
105 K. Yang, Z. Zhao, M. Liu, Z. Zhou, K. Wang, X. Ma, J. Wang, Z. He and F. Zhang, *Chem. Eng. J.*, 2022, **427**, 131802.
106 K. Yang, J. Wang, Z. Zhao, Y. Sun, M. Liu, Z. Zhou, X. Zhang and F. Zhang, *Chem. Eng. J.*, 2022, **435**, 134973.
107 J. Park, J. H. Seo, S. W. Yeom, C. H. Yao, V. W. Yang, Z. Y. Cai, Y. M. Jhon and B. K. Ju, *Adv. Opt. Mater.*, 2018, **6**, 1701140.
108 Y. Wang, T. Hasegawa, H. Matsumoto and T. Michinobu, *J. Am. Chem. Soc.*, 2019, **141**, 3566–3575.
109 M. Kim, W. T. Park, S. A. Park, C. W. Park, S. U. Ryu, D. H. Lee, Y. Y. Noh and T. Park, *Adv. Funct. Mater.*, 2019, **29**, 1805994.
110 J. Park, C. Lee, T. Kim, H. Kim and Y. Kim, *Adv. Electron. Mater.*, 2021, **7**, 2000932.
111 M. J. Kim, S. Choi, M. Lee, H. Heo, Y. Lee, J. H. Cho and B. Kim, *ACS Appl. Mater. Interfaces*, 2017, **9**, 19011–19020.
112 H. J. Chen, G. S. Cai, A. K. Guo, Z. Y. Zhao, J. H. Kuang, L. P. Zheng, L. L. Zhao, J. Y. Chen, Y. L. Guo and Y. Q. Liu, *Macromolecules*, 2019, **52**, 6149–6159.

113 Q. Y. Li, Y. Ran, W. Shi, M. C. Qin, Y. L. Sun, J. H. Kuang, H. L. Wang, H. J. Chen, Y. L. Guo and Y. Q. Liu, *Appl. Mater. Today*, 2021, **22**, 100899.
114 Y. L. Guo, C. Y. Du, G. Yu, C. A. Di, S. D. Jiang, H. X. Xi, J. Zheng, S. K. Yan, C. L. Yu, W. P. Hu and Y. Q. Liu, *Adv. Funct. Mater.*, 2010, **20**, 1019–1024.
115 M. Y. Lee, J. Hong, E. K. Lee, H. Yu, H. Kim, J. U. Lee, W. Lee and J. H. Oh, *Adv. Funct. Mater.*, 2016, **26**, 1445–1453.
116 H. T. Zhang, Y. T. Zhang, X. X. Song, Y. Yu, M. X. Cao, Y. L. Che, Z. Zhang, H. T. Dai, J. B. Yang, G. Z. Zhang and J. Q. Yao, *ACS Photonics*, 2017, **4**, 584–592.
117 H. H. Xu, J. Li, B. H. K. Leung, C. C. Y. Poon, B. S. Ong, Y. T. Zhang and N. Zhao, *Nanoscale*, 2013, **5**, 11850–11855.
118 Z. H. Sun, J. H. Li and F. Yan, *J. Mater. Chem.*, 2012, **22**, 21673–21678.
119 Y. Q. Peng, W. L. Lv, B. Yao, G. Y. Fan, D. Q. Chen, P. J. Gao, M. Q. Zhou and Y. Wang, *Org. Electron.*, 2013, **14**, 1045–1051.
120 G. B. Zhang, J. H. Guo, M. Zhu, P. Li, H. B. Lu, K. Cho and L. Z. Qiu, *Polym. Chem.*, 2015, **6**, 2531–2540.
121 X. T. Liu, Y. L. Guo, Y. Q. Ma, H. J. Chen, Z. P. Mao, H. L. Wang, G. Yu and Y. Q. Liu, *Adv. Mater.*, 2014, **26**, 3631–3636.
122 C. Wang, X. C. Ren, C. H. Xu, B. B. Fu, R. H. Wang, X. T. Zhang, R. J. Li, H. X. Li, H. L. Dong, Y. G. Zhen, S. B. Lei, L. Jiang and W. P. Hu, *Adv. Mater.*, 2018, **30**, 1706260.
123 F. Li, Y. Chen, C. Ma, U. Buttner, K. Leo and T. Wu, *Adv. Electron. Mater.*, 2017, **3**, 1600430.
124 G. H. Wang, K. Q. Huang, Z. Liu, Y. C. Du, X. H. Wang, H. B. Lu, G. B. Zhang and L. Z. Qiu, *ACS Appl. Mater. Interfaces*, 2018, **10**, 36177–36186.
125 J. Kim, J. Kim, S. Jo, J. Kang, J. W. Jo, M. Lee, J. Moon, L. Yang, M. G. Kim, Y. H. Kim and S. K. Park, *Adv. Mater.*, 2016, **28**, 3078–3086.
126 J. Kim, S. M. Kwon, Y. K. Kang, Y. H. Kim, M. J. Lee, K. Han, A. Facchetti, M. G. Kim and S. K. Park, *Sci. Adv.*, 2019, **5**, eaax8801.
127 Y. S. Rim, Y. Yang, S. H. Bae, H. J. Chen, C. Li, M. S. Goorsky and Y. Yang, *Adv. Mater.*, 2015, **27**, 6885.
128 L. T. Dou, Y. Yang, J. B. You, Z. R. Hong, W. H. Chang, G. Li and Y. Yang, *Nat. Commun.*, 2014, **5**, 5404.
129 X. Hu, X. D. Zhang, L. Liang, J. Bao, S. Li, W. L. Yang and Y. Xie, *Adv. Funct. Mater.*, 2014, **24**, 7373–7380.
130 C. Xie and F. Yan, *ACS Appl. Mater. Interfaces*, 2017, **9**, 1569–1576.
131 H. Kim, Z. H. Wu, N. Eedugurala, J. D. Azoulay and T. N. Ng, *ACS Appl. Mater. Interfaces*, 2019, **11**, 36880–36885.
132 D. W. Li, J. Q. Du, Y. J. Tang, K. Liang, Y. Wang, H. H. Ren, R. Wang, L. Meng, B. W. Zhu and Y. F. Li, *Adv. Funct. Mater.*, 2021, **31**, 2105887.
133 Z. G. Zhang and Y. F. Li, *Angew. Chem., Int. Ed.*, 2021, **60**, 4422–4433.
134 H. H. Xu, J. Liu, J. Zhang, G. D. Zhou, N. Q. Luo and N. Zhao, *Adv. Mater.*, 2017, **29**, 1700975.
135 G. B. Zhang, Z. W. Ye, P. Li, J. H. Guo, Q. H. Wang, L. X. Tang, H. B. Lu and L. Z. Qiu, *Polym. Chem.*, 2015, **6**, 3970–3978.
136 A. J. Kronemeijer, E. Gili, M. Shahid, J. Rivnay, A. Salleo, M. Heeney and H. Sirringhaus, *Adv. Mater.*, 2012, **24**, 1558–1565.
137 B. Yang, Y. Lu, D. H. Jiang, Z. C. Li, Y. Zeng, S. Zhang, Y. Ye, Z. Liu, Q. Q. Ou, Y. Wang, S. L. Dai, Y. P. Yi and J. Huang, *Adv. Mater.*, 2020, **32**, 2001227.
138 B. Yang, Y. Wang, L. Li, J. Y. Zhang, J. L. Wang, H. X. Jiao, D. D. Hao, P. Guo, S. Zeng, Z. K. Hua and J. Huang, *Adv. Funct. Mater.*, 2021, **31**, 2103787.
139 G. B. Zhang, J. H. Guo, J. Zhang, W. T. Li, X. H. Wang, H. B. Lu and L. Z. Qiu, *Dyes Pigm.*, 2016, **126**, 20–28.
140 Y. H. He, J. T. E. Quinn, D. L. Hou, J. H. L. Ngai and Y. N. Li, *J. Mater. Chem. C*, 2017, **5**, 12163–12171.
141 H. Han, C. Lee, H. Kim and Y. Kim, *Adv. Funct. Mater.*, 2018, **28**, 1800704.
142 J. W. Suk, W. H. Lee, J. Lee, H. Chou, R. D. Piner, Y. F. Hao, D. Akinwande and R. S. Ruoff, *Nano Lett.*, 2013, **13**, 1462–1467.
143 J. Boonlakhorn, B. Putasaeng, P. Kidkhunthod and P. Thongbai, *Mater. Design*, 2016, **92**, 494–498.
144 A. E. London, L. F. Huang, B. A. Zhang, M. B. Oviedo, J. Tropp, W. C. Yao, Z. H. Wu, B. M. Wong, T. N. Ng and J. D. Azoulay, *Polym. Chem.*, 2017, **8**, 2922–2930.
145 J. Han, J. Qi, X. Zheng, Y. Wang, L. Hu, C. Guo, Y. Wang, Y. Li, D. Ma, W. Qiao and Z. Y. Wang, *J. Mater. Chem. C*, 2017, **5**, 159–165.
146 M. Li, C. An, T. Marszalek, X. Guo, Y.-Z. Long, H. Yin, C. Gu, M. Baumgarten, W. Pisula and K. Muellen, *Chem. Mater.*, 2015, **27**, 2218–2223.
147 H. Shi, C. Liu, Q. Jiang and J. Xu, *Adv. Electron. Mater.*, 2015, **1**, 1500017.
148 S. Cho, J. S. Lee and H. Joo, *Polymers*, 2019, **11**, 1965.
149 N. Massonnet, A. Carella, A. de Geyer, J. Faure-Vincent and J.-P. Simonato, *Chem. Sci.*, 2015, **6**, 412–417.
150 J. Niziol, E. Gondek and K. J. Plucinski, *J. Mater. Sci.: Mater. Electron.*, 2012, **23**, 2194–2201.
151 C. Lee, H. Kim and Y. Kim, *npj Flex. Electron.*, 2021, **5**, 10.